



A study of the electrical and optical properties of AZO thin film by controlling pulse frequency of HiPIMS

Peerapong NUCHUAY^{1,*}, Chinoros LAONGWAN¹, Wimol PROMCHAM¹, Pacharamon SOMBOONSAKSRI², Sukon KALASUNG², Chanunthorn CHANANONNAWATHORN², Pitak EIAMCHAI², Viyapol PATTHANASETTAKUL², Chamnan PROMJANTUK³, Kittikhun SEAWSAKUL⁴, Noppadon NUNTAWONG², Mati HORPRATHUMB², and Saksorn LIMWICHEAN^{2,*}

¹Program of Industrial Electrical Technology, Faculty of Science and Technology, Suratthani Rajabhat University, Mueang, Surat Thani, 841000, Thailand

²National Electronics and Computer Technology Center (NECTEC), National Science and Technology Development Agency, Pathum Thani, 12120 Thailand

³Department of physics, Faculty of Science and Technology, Nakhon Ratchasima Rajabhat University, Nakhon Ratchasima Province, 30000, Thailand

⁴Educational Research Development and Demonstration Institute, Srinakharinwirot University, Ongkharak, Nakhon Nayok Province, 26120, Thailand

*Corresponding author e-mail: deva.drr@gmail.com

Received date:

7 October 2022

Revised date

16 March 2023

Accepted date:

17 March 2023

Keywords:

AZO thin film;
HiPIMS;
Pulse frequency;
Transparent conductive oxides

Abstract

The transparent conductive oxide (TCO) which is AZO thin film was prepared by controlling pulse frequency at 100 Hz to 900 Hz using high-power impulse magnetron sputtering (HiPIMS). All samples were deposited on silicon (100) and glass slide substrates which the thickness was kept constant at 400 nm. The surface morphology was investigated by field-emission scanning electron microscope (FE-SEM), crystallinity by Grazing Incidence X-ray Diffraction (GI-XRD), optical transparency by UV-Vis-NIR spectrophotometry, and electrical properties using Hall effect instrument. It was found that the AZO films exhibited dense columnar structure. The GI-XRD patterns of AZO films demonstrated the crystal growth direction which was preferred the hexagonal wurtzite structure at (002) and (103) planes. The AZO film prepared by using 700 Hz of frequency (duty cycle 7%) showed the average visible transmittance (T_{avg}) at 82% in the visible region (380 nm to 780 nm). Additionally, the resistivity, high mobility and carrier concentration of AZO film were found to be $3.0 \times 10^{-3} \Omega \cdot \text{cm}^{-1}$, $10.53 \text{ cm}^2 \cdot \text{Vs}^{-1}$ and $1.82 \times 10^{20} \cdot \text{cm}^{-3}$, respectively. The fabrication of AZO film presented excellent electrical and optical properties which could be applied in several optoelectronic applications.

1. Introduction

Transparent conductive oxides (TCOs) have received much attention due to their promising electrical and optical properties. The TCO materials exhibit their relatively low resistivity of $10^{-3} \Omega \cdot \text{cm}^{-1}$ to $10^{-4} \Omega \cdot \text{cm}^{-1}$ and high transmittance in the visible range at around 80% [1]. Therefore, it could be utilized in various applications, especially in thin film-based optoelectronic for the manufacture of photovoltaic cells, organic light-emitting devices, transparent electrodes, infrared optical windows, touch panels and flat screens [2-5]. Several doped metal oxides have been applied to TCO materials to enhance their electrical properties such as indium doped tin oxide (ITO), fluorine doped tin oxide (FTO) and aluminum doped zinc oxide (AZO). Among these materials, ITO is the most favorable because of its low resistivity and high transparent in visible region. However, the utilization of ITO material was limited due to its high cost and lack of availability of indium which could be replaced by non-toxic materials. In particular,

the AZO is of interest as an alternative for the ITO because of the good electrical property, less toxic, cost-effective, high transmittance in visible region, as well as high thermal stability [6-8]. Additionally, AZO thin films can be fabricated using several techniques including sol-gel process [9], chemical spray deposition [10], chemical vapor deposition (CVD) [11], pulsed laser deposition (PLD) [12], and DC and/or RF magnetron sputtering [13-15]. Among these deposition methods, the DC magnetron sputtering technique provides a uniform distribution of the deposited thin films and allows the possibilities of the deposition of large surface area on different types of substrates. Nevertheless, the plasma ionization of DC magnetron sputtering was generally low, resulting in low adhesion and less homogeneous of thin film. Therefore, an alternative technique is a high-power impulse magnetron sputtering (HiPIMS), which offers a sputtering power at extremely high levels of more than $1000 \text{ W} \cdot \text{cm}^{-2}$ in short pulses (impulses) of tens of microseconds at low duty cycle (on/off time ratio) of <10% [16-19]. In general, HiPIMS was successfully used towards

highly ionized metal plasma with high plasma densities in the order of 10^{19} m^{-3} [16,19-21]. The energy of ions can be enhanced corresponding to the ultra-short pulse on time of HiPIMS which results in increasing kinetic energy of sputtered atoms and high ad-atom mobility during the film growth. Hence, the coated film typically presents high crystalline quality, well adhesion, and high packing density when compared to DC magnetron sputtering [22-24]. Thus, in this work, we investigated the influence of pulse frequency on surface morphology, crystalline structure, optical and electrical property of AZO thin films which was deposited using HiPIMS.

2. Experimental

The AZO thin films were deposited on Si wafer (100) and glass substrates. The glass substrates were cleaned by acetone, Isopropanol and DI water using an ultrasonic bath for 15 min of each step. Then the substrates were dried in nitrogen flow, followed by heating at 80°C for 10 min in a furnace. Consequently, the high-power impulse magnetron sputtering (HiPIMS) (Ionautics HIPITER1) was operated using sputtering average power of 100 watts and pulse frequency at 100 Hz to 900 Hz. The pulse width was kept constant at $100 \mu\text{s}$, as shown in Figure 1. The ZnO-Al (2 wt%) target (Kurt Lesker), 3 inches, was used as the source material. All of the samples were deposited with controlled substrate rotation at 10 rpm. Inside the chamber, the base pressure was 5×10^{-6} mbar and working gas argon flow was fixed at 3.0×10^{-3} mbar. The target was pre-sputtered for 2 min before coating. In addition, the film thickness at 400 nm was controlled by adjusting the deposition time which corresponding to the deposition rate of each condition. The deposition rate was firstly examined by

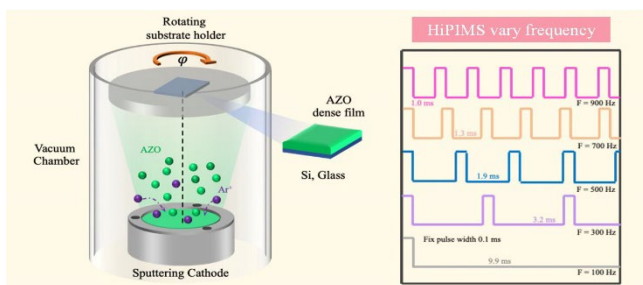


Figure 1. Schematic representation of AZO thin film deposition using HiPIMS in the pulse frequency of 100 Hz to 900 Hz.

keep the deposition time constant at 30 min. The obtained thickness was then used to calculate to provide the deposition rate of each sputtering condition. The crystal structures of the AZO thin films were investigated by XRD (Cu K α radiation, KTTRAXIII, Rigaku). The physical morphologies were observed by FESEM (SU8030, Hitachi). The optical transmission was determined by UV-Vis-NIR spectrophotometer (Cary 7000, Agilent) in the wavelength of 200 nm to 2000 nm. In addition, the electrical properties were characterized by Hall-effect measurements at room temperature using a Ecopia HMS-3000 system.

3. Results and discussion

The AZO thin films were deposited using HiPIMS at a pulse width of $100 \mu\text{s}$ of varied pulse frequencies in the range of 100 Hz to 900 Hz. Table 1 lists the value of pulse frequency, duty cycle, average voltage, peak current, average current, and average power during the deposition of AZO thin films. The voltage varies from 578 V to 442 V and the peak current varies from 47 A to 2 A as duty cycle increased from 1% to 9%. It was indicated that the lower plasma ionization was a consequence of the increase of duty cycle [25,26]. In order to avoid the influence of the film thickness on the properties of the films, all AZO thin films were prepared at the thicknesses of 400 nm and presented similar grain size, as shown in Figure 2(a). In addition, the results indicated that as the pulse frequency increased, the deposition rate was also increased (Figure 2(b)). This result also corresponded to Bradley *et al.*, which reported that as increased duty cycle, the deposition rate was increased as well [26,27].

Figure 3 shows the XRD patterns of AZO films deposited on Si substrates at different pulse frequencies. The diffraction peaks indicated that the films had polycrystalline structures, which could be characterized as a wurtzite structure and corresponded to the (002) plane at 34.46° and the (103) plane at 62.81° [8,14]. The varying intensity of diffraction peak at different pulse frequencies was also observed, showing that the peak of (103) plane increased at the higher frequency. Additionally, the shift in diffraction peak was found which was attributed to the change of residual stress in thin film inducing by the reduced ion bombardment at high pulse frequency [28,29]. In contrast, the peak of (002) plane was slightly decreased. This suggested that the growth of crystal structure of AZO film was increased along the a-axis.

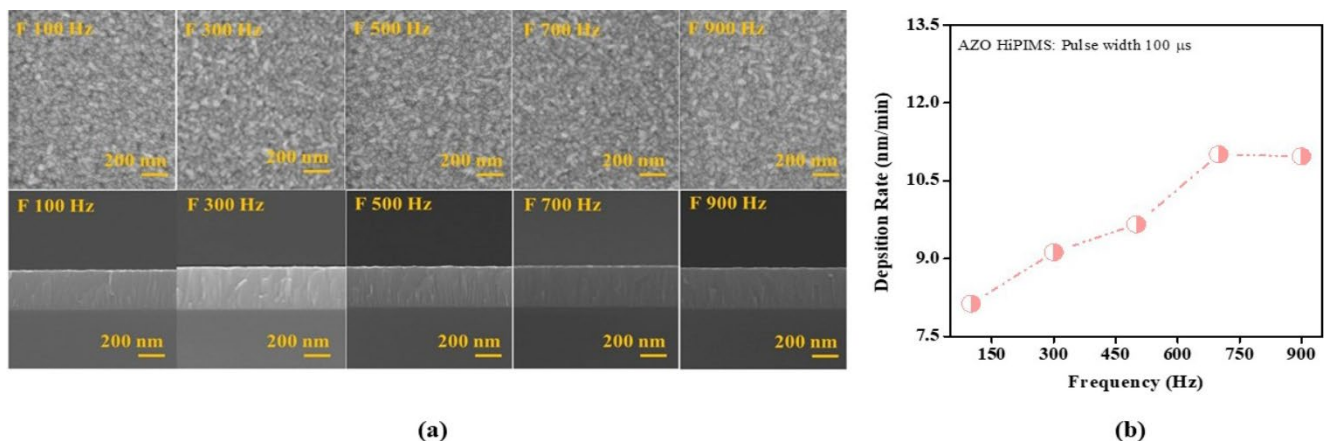


Figure 2. (a) FE-SEM images of surface and cross-section of AZO thin films prepared by HiPIMS. (b) The deposition rate as a function of pulse frequency.

Table 1. Pulse frequency, duty cycle, average voltage, peak current, and average current during the deposition of AZO thin films.

Pulse frequency (Hz)	Duty cycle (%)	Average voltage (V)	Peak current (A)	Average current (A)
100	1	578	47	0.174
300	3	508	8	0.198
500	5	468	4	0.213
700	7	455	3	0.220
900	9	442	2	0.225

The optical property of the prepared AZO thin films on glass slide substrate using HiPIMS was investigated. The transmission spectra were performed in the range of 300 nm to 1800 nm at normal incidence via UV-Vis-NIR spectrophotometer as shown in Figure 4. The similar optical interference and high transparency of the prepared AZO thin films was observed. The results indicated the nearly identical of all samples. For direct comparison, the average transmittance (T_{avg}) of the samples was calculated from integral visible transmittance in the visible region (380 nm to 780 nm) [23,30]. It was found that as pulse frequency increased, the T_{avg} of AZO thin films was also increased. Additionally, the maximum T_{avg} of AZO thin films presented at 82.61% of 700 Hz and dropped to 80.08% at 900 Hz.

The electrical properties of the AZO films have been measured using the Hall effect. Figure 5 shows the decreasing resistivity of the AZO films from $5.4 \times 10^{-3} \Omega \cdot \text{cm}^{-1}$ to $3.0 \times 10^{-3} \Omega \cdot \text{cm}^{-1}$ when the pulse frequencies were operated to 700 Hz, and then slightly increased at 900 Hz. The higher carrier concentration and mobility were exhibited at pulse frequency of 100 Hz to 700 Hz. The maximum carrier concentration and mobility value of $1.82 \times 10^{20} \text{ cm}^{-3}$ and $10.53 \text{ cm}^2 \cdot \text{Vs}^{-1}$ were also displayed at the pulse frequencies of 700 Hz. Generally, AZO was n-type material which its electron donor could be optimized through the Al-doping level [31,32]. This could be implied that the HiPIMS pulse frequency affected directly to the carrier concentration and donor level. In addition, the good electrical conductivity with reasonable low optical loss can be provided for

this work [33]. These results corresponded to the most prominent peak at (103) plan of AZO which was higher when the pulse frequency was increased. This is in agreement with previous reports indicating the incorporation of Al as a dopant in ZnO lattice [33,34].

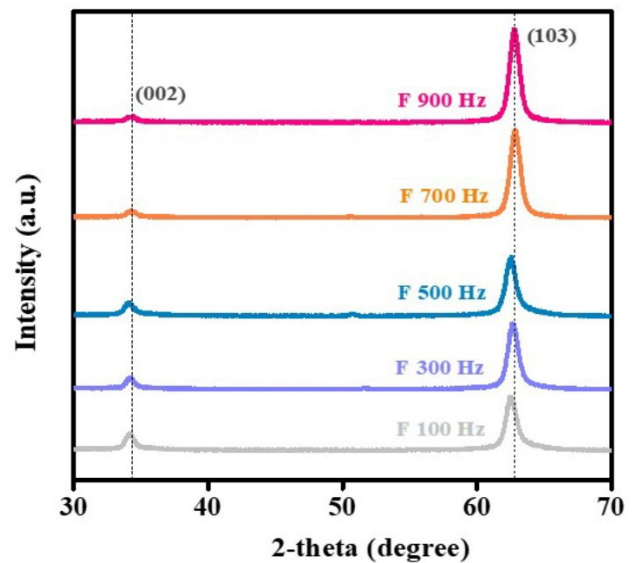


Figure 3. XRD patterns of the AZO thin films that were deposited on silicon substrates.

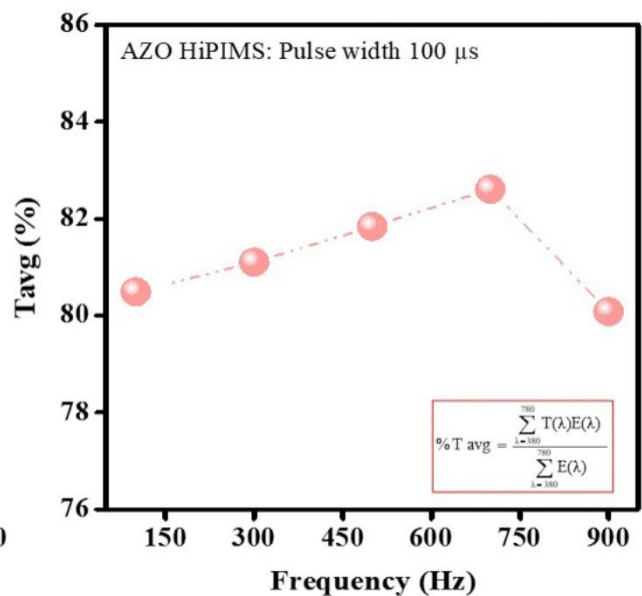
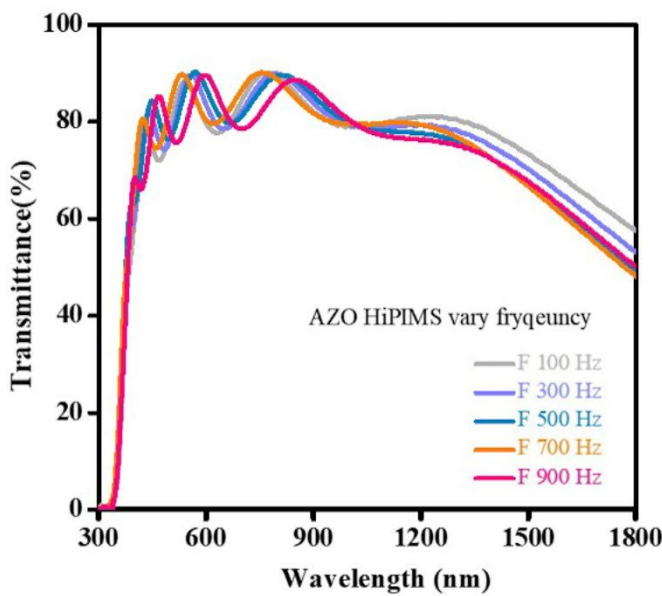


Figure 4. (a) UV-visible light transmittance and (b) transmittance average of the AZO thin films that were deposited on glass substrates

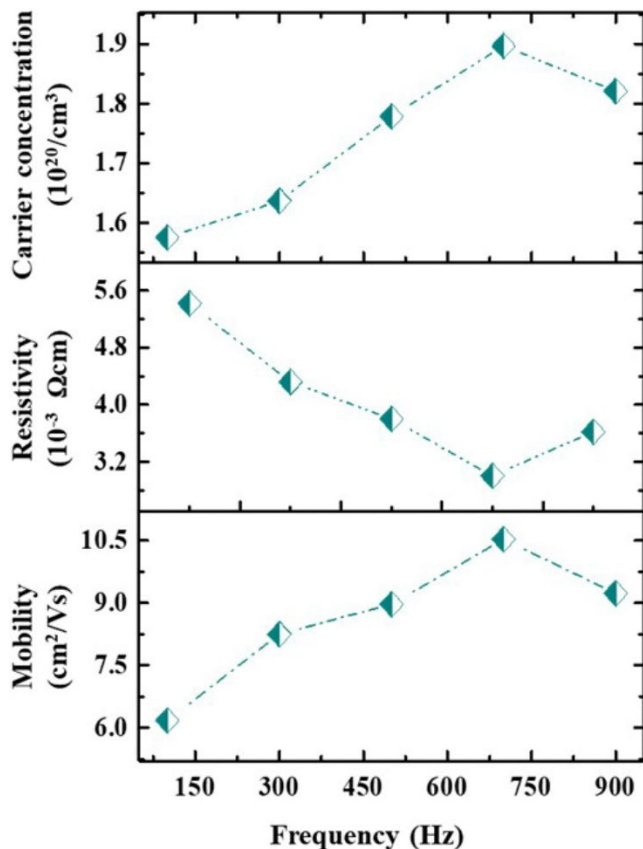


Figure 5. Hall effect as a function of AZO thin film including carrier concentration resistivity and mobility.

4. Conclusion

The AZO thin film using HiPIMS deposition technique was successfully fabricated. It was found that by varying pulse frequency of 100 Hz to 900 Hz (duty cycle 1% to 9.1%), the deposition rate was increased leading to increasing crystallinity of obtained AZO films. This work demonstrated that the preparation of AZO thin film using HiPIMS at very low duty cycle was inappropriate resulting in the higher resistivity. The optimal condition at 7.1% of duty cycle at 700 Hz of pulse frequency provided the highest transparency and conductivity of thin film. Therefore, it could be practically applied to various optoelectronic applications.

References

- [1] M. Mohamedi, F. Challali, T. Touam, A. Chelouche, S. Ouhenia, A. H. Souici, and D. Djouadi, "AZO thin films grown by confocal RF sputtering: role of deposition time on microstructural, optical, luminescence and electronic properties," *Journal of Materials Science: Materials in Electronics*, vol. 32, pp. 25288-25299, 2021.
- [2] M. Asemi, M. Ahmadi, and M. Ghanaatshoar, "Preparation of highly conducting Al-doped ZnO target by vacuum heat treatment for thin film solar cell applications," *Ceramics International*, vol. 44, pp. 12862-12868, 2018.
- [3] H. Kim, A. Pique, J.S. Horwitz, H. Murata, Z.H. Kafafi, C.M. Gilmorea, and D.B. Chrisey, "Effect of aluminum doping on zinc oxide thin films grown by pulsed laser deposition for organic light-emitting devices," *Thin Solid Films*, vol. 377, pp. 798-802, 2000.
- [4] T. Minami, "Transparent conducting oxide semiconductors for transparent electrodes. Semicond," *Semiconductor Science and Technology*, vol. 20, pp. 35-44, 2005.
- [5] R. A. Afre, N. Sharma, and M. Sharon, "Transparent conducting oxide films for various applications: A review," *Reviews on Advanced Materials Science*, vol. 53, pp. 79-89, 2018.
- [6] K. Seawsakul, M. Horprathum, P. Eiamchai, V. Pattantsetakul, S. Limwichean, P. Muthitamongkol, C. Thanachayanont, and P. Songsiririthigul, "Transparent conductive nanocolumnar AZO film coating by glancing angle deposition technique," *AIP Conference Proceedings 2010*, 020017, 2018.
- [7] K. Yim, and C. Lee, "Optical properties of Al-doped ZnO thin films deposited by two different sputtering methods," *Crystal Research and Technology*, vol. 41, pp. 1198-1202, 2006.
- [8] A. V. Singh, M. Kumar, R.M. Mehra, A. Wakahara, and A. Yoshida, "Al-doped zinc oxide (ZnO: Al) thin films by pulsed laser ablation," *Journal of the Indian Institute of Science*, vol. 81, pp. 527-533, 2001.
- [9] K. Necib, T. Touam, A. Chelouche, L. Ouarez, D. Djouadi, and B. Boudine, "Investigation of the effects of thickness on physical properties of AZO sol-gel films for photonic device applications," *Journal of Alloys and Compounds*, vol. 735, pp. 2236-2246, 2018.
- [10] M. Humayan Kabir, M. Mintu Ali, M. Abdul Kaiyum, and M.S. Rahman, "Effect of annealing temperature on structural morphological and optical properties of spray pyrolyzed Al-doped ZnO thin films," *Journal of Physics Communications*, vol. 3, pp. 105007, 2019.
- [11] S. Saini, P. Mele, T. Oyake, J. Shiomi, J.-P. Niemela, M. Karppinen, K. Miyazaki, C. Li, T. Kawaharamura, and A. Ichi-nose, "Porosity-tuned thermal conductivity in thermoelectric Al-doped ZnO thin films grown by mist-chemical vapor deposition," *Thin Solid Films*, vol. 685, pp. 180-185, 2019.
- [12] L. Ma, X. Ai, H. Quan, W. Yang, and X. Du, "Resistivity depends on preferred orientation for transparent conductive thin films," *Journal of the Korean Physical Society*, vol. 74, pp. 806-811, 2019.
- [13] Y. Xia, P. Wang, S. Shi, M. Zhang, G. He, J. Lv, and Z. Sun, "Deposition and characterization of AZO thin films on flexible glass substrates using DC magnetron sputtering technique," *Ceramics International*, vol. 43, pp. 4536-4544, 2017.
- [14] K. Seawsakul, M. Horprathum, P. Eiamchai, V. Pattantsetakul, S. Limwichean, P. Muthitamongkol, C. Thanachayanont, and P. Songsiririthigul, "Effects of sputtering power toward the Al-doped ZnO thin Film prepared by pulsed DC magnetron sputtering," *Materials Today: Proceedings*, vol. 4, pp. 6466-6471, 2017.
- [15] D. Mendil, F. Challali, T. Touam, V. Bockelée, S. Ouhenia, A. Souici, D. Djouadi, and A. Chelouche, "Preparation of RF sputtered AZO/Cu/AZO multilayer films and the investigation of Cu thickness and substrate effects on their microstructural and optoelectronic properties," *Journal of Alloys and Compounds*, vol. 860, pp. 158470, 2020.

- [16] V. Kouznetsov, K. Macak, J. M. Schneider, U. Helmersson, and I. Petrov, "A novel pulsed magnetron sputter technique utilizing very high target power densities," *Surface and Coatings Technology*, vol. 122, pp. 290-293, 1999.
- [17] D. V. Mozgrin, I. K. Fetisov, and G. V. Khodachenko, "High-current low-pressure quasi-stationary discharge in a magnetic field: experimental research," *Plasma Physics Reports*, vol. 21, pp. 400-409, 1995.
- [18] S. P. Bugaev, N. N. Koval, N. S. Sochugov, and A. N. Zakharov, "Investigation of a high-current pulsed magnetron discharge initiated in the low-pressure diffuse arc plasma," *Proceedings of 17th International Symposium on Discharges and Electrical Insulation in Vacuum*, vol. 2, pp. 1074-1076, 1996.
- [19] K. Macák, V. Kouznetsov, J. Schneider, U. Helmersson, and I. Petrov, "Ionized sputter deposition using an extremely high plasma density pulsed magnetron discharge," *Journal of Vacuum Science & Technology A*, vol. 18, pp. 1533-1537, 2000.
- [20] A. P. Ehasarian, R. New, W. D. Munz, L. Hultman, U. Helmersson, and V. Kouznetsov, "Influence of high power densities on the composition of pulsed magnetron plasmas," *Vacuum*, vol. 65, pp. 147-154, 2002.
- [21] J. T. Gudmundsson, J. Alami, and U. Helmersson, "Evolution of the electron energy distribution and plasma parameters in a pulsed magnetron discharge," *Applied Physics Letters*, vol. 78, pp. 3427-3429, 2001.
- [22] S. Kment, P. Schmuki, Z. Hubicka, L. Machala, R. Kirchgeorg, N. Liu, and L. Wang, K., "Efficiency of thin hematite films exhibiting solely (110) crystal orientation," *ACS Nano*, vol. 9, pp. 7113-7123, 2015.
- [23] S. Limwichean, P. Eiamchai, P. Chatchai, N. Kasayapanand, and M. Horprathum, "Comparative investigations of DCMS/HiPIMS reactively sputtered WO₃ thin films for photo-electrochemical efficiency enhancements," *Vacuum*, vol. 185, pp. 109978, 2021.
- [24] U. Helmersson, M. Lattemann, J. Bohlmark, A. P. Ehasarian, and J. T. Gudmundsson, "Review Ionized physical vapor deposition (IPVD): A review of technology and applications," *Thin Solid Films*, vol. 513, pp. 1-24, 2006.
- [25] C-L. Chang, G-J. Luo, F-C. Yang, and J-F. Tang, "Effects of duty cycle on microstructure of TiN coatings prepared using CAE/HiPIMS," *Vacuum*, vol. 192, p. 110449, 2021.
- [26] C-L. Chang, S-G. Shih, P-H. Chen, W-C. Chen, C-T. Ho, and W-Y. Wu, "Effect of duty cycles on the deposition and characteristics of high power impulse magnetron sputtering deposited TiN thin films," *Surface & Coatings Technology*, vol. 259, pp. 232-237, 2014.
- [27] J. W. Bradley, A. Mishra, and P. J. Kelly, "The effect of changing the magnetic field strength on HiPIMS deposition rates," *Journal of Physics D: Applied Physics*, vol. 48, p. 215202, 2015.
- [28] K. Seawsakul, M. Horprathum, P. Eiamchai, V. Pattantsetakul, S. Limwichean, C. Chananonwathorn, P. Muthitamongkol, C. Thanachayanont, A. Klamchuen, T. Wutikhun, H. Nakajima, M. Sripakdee, and P. Songsiriritthigul, "Influence of vacuum annealing temperature on structural, optical and electrical of nanocolumnar AZO films for TCO application," *Chiang Mai Journal of Science*, vol. 47, no. 4, pp. 815-822, 2020.
- [29] H. Mei, J. C. Ding, X. Xiao, Q. Luo, R. Wang, Q. Zhang, W. Gong, and Q. Wang, "Influence of pulse frequency on microstructure and mechanical properties of Al-Ti-V-Cu-N coatings deposited by HiPIMS," *Surface and Coatings Technology*, vol. 205, p. 126514, 2021.
- [30] X. Lv, Y. Cao, L. Yan, Y. Li, Y. Zhang, and L. Song, "Atomic layer deposition of V_{1-x}MoxO₂ thin films, largely enhanced luminous transmittance, solar modulation," *ACS Appl. Mater. Interfaces*, vol. 10, pp. 6601-6607, 2018.
- [31] Y. K. Tseng, G. J. Gao, and S. C. Chien. "Synthesis of c-axis preferred orientation ZnO:Al transparent conductive thin films using a novel solvent method." *Thin Solid Films*, vol. 518, pp. 6259-6263, 2010.
- [32] F. Khan, Vandana, S. N. Singh, M. Husain, and P. K. Singh. "Sol-gel derived hydrogen annealed ZnO:Al films for silicon solar cell application." *Sol. Energy. Mater. Sol. Cells*, vol. 100, pp. 57-60, 2012.
- [33] Z. Lamia, T. Touam, D. Vrel, N. Souded, S. B. Yahia, O. Brinza, A. Fischer, and A. Boudrioua. "AZO thin films by sol-gel process for integrated optics." *Coatings*, vol. 3, pp. 126-139, 2013.
- [34] P. Muthitamongkol, C. Thanachayanont, B. Samransuksamer, K. Seawsakul, M. Horprathum, P. Eiamchai, S. Limwichean, V. Patthanasettakul, N. Nuntawong, P. Songsiriritthiguland, and P. Chindaudom, "The effects of the argon plasma treatments on transparent conductive aluminum-doped zinc oxide thin films prepared by the pulsed DC magnetron sputtering," *Materials Today: Proceedings*, vol. 4, pp. 6248-6253, 2017.
- [35] Q. J. Jiang, J. G. Lu, Y. L. Yuan, L. W. Sun, X. Wang, Z. Wen, Z. Z. Ye, D. Xiao, H. Z. Ge, and Y. Zhao, "Tailoring the morphology, optical and electrical properties of DC-sputtered ZnO:Al films by post thermal and plasma treatments," *Materials Letters*, vol. 106, pp. 125-128, 2013.